

# The structures of poly(oxyethylene)s having sulfone groups in the side chains

S.-Y. Park<sup>a</sup>, B.L. Farmer<sup>a,\*</sup>, J.-C. Lee<sup>b</sup>

<sup>a</sup>Air Force Research Laboratory, Materials and Manufacturing Directorate, Wright-Patterson Air Force Base, OH, 45433-7750, USA

<sup>b</sup>School of Chemical Engineering, Seoul National University, Seoul 151-744, South Korea

Received 18 December 2000; received in revised form 27 July 2001; accepted 31 July 2001

## Abstract

The structures of  $(-\text{OCH}_2\text{CHR}-)$  with  $\text{R} = \text{CH}_2\text{S}(\text{CH}_2)_6\text{SO}_2(\text{CH}_2)_M\text{H}$  (ATP- $M$ ;  $M = 5, 7, 9$ ) or  $\text{R} = \text{CH}_2\text{SO}_2(\text{CH}_2)_6\text{SO}_2(\text{CH}_2)_M\text{H}$  (ASP- $M$ ;  $M = 5, 7, 9$ ) were studied using X-ray diffraction and differential scanning calorimetry. The X-ray patterns of all ATPs and ASPs studied show a series of ordered reflections in the small angle region and a sharp wide angle reflection at  $d = \sim 4.4 \text{ \AA}$ , characteristic of a smectic phase. The smectic layer thickness corresponds to twice the most extended side chain length and linearly increases as the side chain length increases with a slope of  $\sim 2.3 \text{ \AA}$  per methylene spacer. This indicates that all ASPs and ATPs studied have a double layer structure with side chains normal to the main chain and probably an all-*trans* conformation of the side chains. The correlation lengths measured from the wide angle reflections are in the range of  $80 \pm 10 \text{ \AA}$  for all the polymers except for ASP-5 ( $\sim 40 \text{ \AA}$ ). These values indicate that quasi-long-range order exists in the smectic layers whose structures can be defined as smectic B ( $S_B$ ). The d-spacing of the wide angle reflection,  $4.4 \text{ \AA}$ , suggests that paraffinic side chain crystallization does not occur and that the smectic mesophase develops through dipole–dipole interactions of sulfone groups in the side chains. During heating, ATP-5 shows recrystallization after the first melting. The structure produced during recrystallization has a similar smectic structure but with more dense packing between side chains than before the first melting. In the case of ASP-9, a smectic to smectic transition was observed at  $\sim 110^\circ\text{C}$  prior to the isotropic temperature at  $\sim 150^\circ\text{C}$ . Both the correlation length (from the wide angle reflection) and the layer thickness decreased from  $\sim 80$  to  $\sim 30 \text{ \AA}$  and from  $46$  to  $40 \text{ \AA}$  at this transition, respectively, indicating that the order in the smectic layers is lost and the  $S_B$  structure has become a less ordered  $S_A$  structure at this transition. © 2001 Elsevier Science Ltd. All rights reserved.

**Keywords:** X-ray diffraction; Poly(oxyethylene); Liquid crystal

## 1. Introduction

Polymers containing *n*-alkyl side chains can form mesophases through side chain crystallization [1–13]. Kaufman et al. discovered in 1948 that polymers containing long paraffinic side groups give rise to side chain crystallization [13]. Since then, many researchers have reached the conclusion that a critical side-chain length (typically eight to nine methylene groups) is required, that the section of the side chain beyond that critical side-chain length participates in crystallization, and that the crystallites are well formed irrespective of the main-chain conformation [6,7]. A sharp reflection at  $d = \sim 4.17 \text{ \AA}$  is found in the X-ray diffraction patterns for most polymers having *n*-alkyl side chains, such as poly(*n*-alkylmethacrylate)s, poly(*n*-alkylacrylate)s, poly(*n*-alkylethylene)s, poly(*n*-alkylethylene oxide)s, poly-

(vinyl *n*-alkyl ester)s, poly(*n*-alkyl acrylamide)s and so on [3,8,11,14,15]. This d-spacing is similar to the spacing observed in the hexagonal modification of crystals of normal paraffins and this reflection is therefore attributed to hexagonal packing of the *n*-alkyl side chains in these polymers.

Some polymers containing *n*-alkyl side chains can form mesophases in other ways. For example, poly(*n*-alkylethylene sulfone)s have side chains attached at every third atom of the polymer backbone and have polar sulfone groups in the main chain. These polymers show a rather broad wide angle reflection at  $d = 4.5\text{--}4.9 \text{ \AA}$  and sharp reflections (multiple orders) in the small angle region [11,16]. This spacing ( $4.5\text{--}4.9 \text{ \AA}$ ) indicates that the mesophase does not develop through the crystallization of the *n*-alkyl side chains. Poly(*n*-alkylethylene oxide)s, which have a chemical structure analogous to poly(*n*-alkylethylene sulfone)s with an oxygen atom replacing the sulfone moiety, show a single, sharp reflection at  $d = 4.12 \text{ \AA}$  [11]. This

\* Corresponding author. Tel.: +1-937-255-9209; fax: +1-937-255-9157.  
E-mail address: barry.farmer@afml.af.mil (B.L. Farmer).

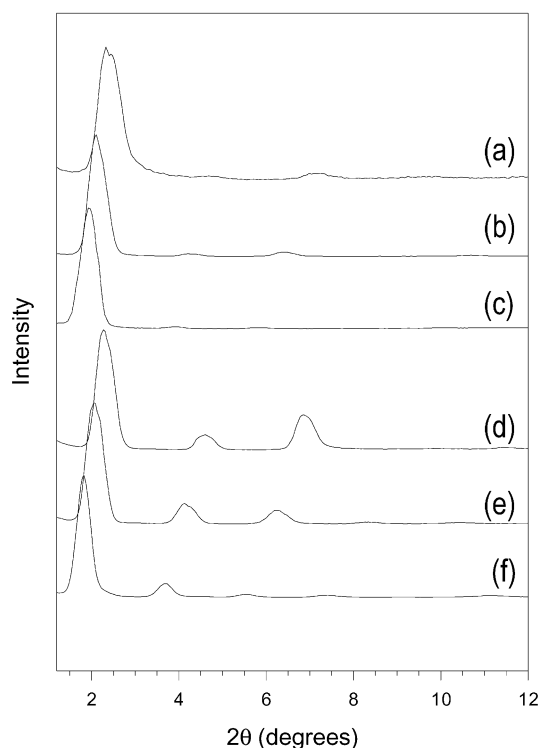


Fig. 1. X-ray powder patterns of (a) ASP-5, (b) ASP-7, (c) ASP-9, (d) ATP-5, (e) ATP-7, and (f) ATP-9 in the small angle region.

difference between poly(*n*-alkylethylene sulfone)s and poly(*n*-alkylethylene oxide)s might be due to the steric and polar character of the SO<sub>2</sub> group, compared with that of an oxygen atom. The main chains of the two polymers probably experience very different intra- and intermolecular interactions, which in turn influence the packing of the side chains.

The synthesis and properties of poly[oxy(*n*-alkylsulfonyl methyl)ethylenes] (–OCH<sub>2</sub>CHR–; R = CH<sub>2</sub>SO<sub>2</sub>(CH<sub>2</sub>)<sub>*N*</sub>H) (ASE-*N*) were reported by Lee et al. [17]. The ASE series contains the very polar sulfone group (4.5 D) in the side chains and has ordered liquid crystalline phases for polymers having moderate alkyl side chains (*N* = 5, 8) while polymers having shorter alkyl side chains (*N* = 1–4) are entirely amorphous. Fiber X-ray patterns showed a series of sharp ordered equatorial reflections and a broad reflection at *d* = ~4.5 Å, which had increased intensity on the meridian, characteristic of an ordered smectic A (S<sub>A</sub>) material. It was suggested that the interactions between sulfone groups may induce the *n*-alkylsulfonyl side chains to form an ordered phase even though the side chains are short.

Recently, other poly(oxyethylene)s with side chain structures such as –CH<sub>2</sub>S(CH<sub>2</sub>)<sub>6</sub>SO<sub>2</sub>(CH<sub>2</sub>)<sub>*M*</sub>H (ATP-*M*) and –CH<sub>2</sub>SO<sub>2</sub>(CH<sub>2</sub>)<sub>6</sub>SO<sub>2</sub>(CH<sub>2</sub>)<sub>*M*</sub>H (ASP-*M*) have been successfully synthesized [18,19]. The ASP series contains two sulfone groups in the side chain while the ATP series has one thioether and one sulfone group in the side chain. Here, we report the structures of ATP-5, 7, and 9 and ASP-5, 7, and 9.

Table 1

The room temperature d-spacings and correlation lengths (*L*) determined from the first reflection in the small angle region and from the wide angle reflection

|       | Small angle   |              | Wide angle    |              |
|-------|---------------|--------------|---------------|--------------|
|       | d-spacing (Å) | <i>L</i> (Å) | d-spacing (Å) | <i>L</i> (Å) |
| ATP-5 | 38.7 ± 0.5    | 233 ± 10     | 4.43 ± 0.02   | 96 ± 3       |
| ATP-7 | 42.1 ± 0.5    | 239 ± 10     | 4.35 ± 0.02   | 75 ± 3       |
| ATP-9 | 48.0 ± 0.5    | 285 ± 10     | 4.32 ± 0.02   | 82 ± 3       |
| ASP-5 | 37.5 ± 0.5    | 184 ± 10     | 4.50 ± 0.02   | 43 ± 3       |
| ASP-7 | 41.9 ± 0.5    | 232 ± 10     | 4.49 ± 0.02   | 74 ± 3       |
| ASP-9 | 46.1 ± 0.5    | 239 ± 10     | 4.47 ± 0.02   | 72 ± 3       |

## 2. Experimental

The synthesis and general characterization of the specimens of ATP-*M*s and ASP-*M*s were reported previously [18,19]. The number average molecular weight ( $\bar{M}_n$ )/polydispersity index of ATP-5, -7, and -9 were 65,000/2.75, 78,000/3.56, and 69,000/3.65, respectively, and those of ASP-5, -7, and -9 were 36,000/3.05, 42,000/2.80, and 30,000/2.6, respectively. (Polystyrene standards were used in the calculation of the molecular weight.) Fiber specimens for X-ray study were prepared by drawing (with tweezers) the isotropic melt on a slide glass. Wide angle X-ray diffraction patterns were recorded on both Kodak Direct Exposure film and a phosphor image plate (Molecular Dynamics®) in a Statton camera. Monochromatic CuK<sub>α</sub> radiation from a rotating anode X-ray generator operating at 40 KV and 240 mA was used. The sample to film distance was calibrated by SiO<sub>2</sub> powders. X-ray patterns at high temperatures were obtained using a heating accessory for the Statton camera. Correlation lengths were estimated using the Scherrer equation, wherein the peak width at half-height of each reflection is reciprocally proportional to the correlation length perpendicular to the reflection planes [20,21].

DSC experiments were carried out in a Perkin–Elmer DSC-7. The temperature and heat flow scales were calibrated using standard materials. The sample size was ~1.5 mg.

## 3. Results and discussion

### 3.1. Smectic structures

Fig. 1 shows the X-ray powder patterns of the ASPs and ATPs in the small angle region. A series of ordered reflections was observed. These reflections indicate that these polymers have highly ordered smectic layered structures, with their thickness corresponding to the d-spacing of the first small angle peak as listed in Table 1. The thickness increases as the side chain length increases (discussed below). Fig. 2 shows the wide angle region of the powder patterns (note: the intensity scale is expanded ~10×

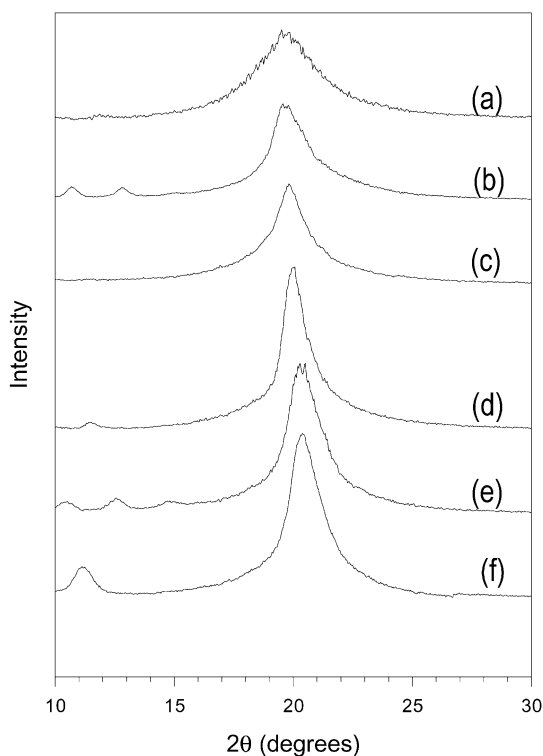


Fig. 2. X-ray powder patterns of (a) ASP-5, (b) ASP-7, (c) ASP-9, (d) ATP-5, (e) ATP-7, and (f) ATP-9 in the wide angle region. (Intensity scale is expanded  $\sim 10\times$  compared with Fig. 1.)

compared with Fig. 1). A single sharp reflection was observed for each polymer with d-spacings in the range of 4.3–4.5 Å, as listed in Table 1. ASPs values are systematically larger, probably due to the presence of the second sulfone groups. These d-spacings do not correspond simply to crystallization of the *n*-alkyl side chains. The strong dipole–dipole interactions between sulfone groups in the side chains may prevent crystallization of the *n*-alkyl side

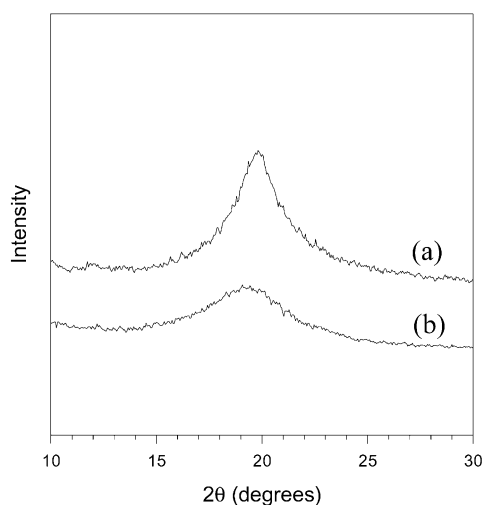


Fig. 3. X-ray powder patterns of ASP-5 at (a) 75°C and (b) 120°C.

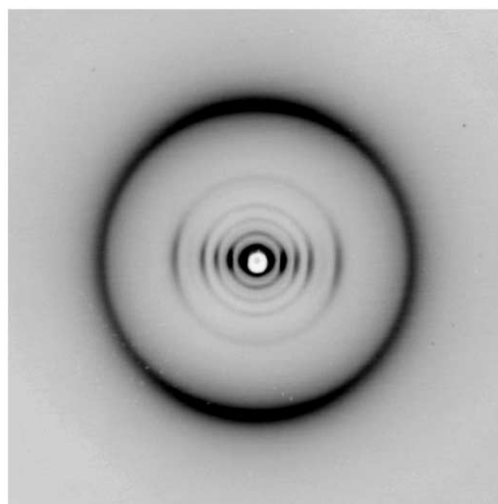


Fig. 4. The X-ray fiber pattern of ATP-9.

chains into a paraffinic structure yet still induce smectic mesophase formation.

The degree of order in the smectic layers can be quantified by examining the width of the 4.4 Å reflection. Typically, smectic A or C phases have short-range order in the layers and their correlation lengths are less than 30 Å [20,21]. More ordered smectic structures can have either quasi-long-range order (correlation length  $\approx 30$ –90 Å) or long-range order (correlation length  $> 100$  Å). The ASP and ATP polymers have correlation lengths between 30 and 100 Å, consistent with quasi-long-range order in the layers. ATPs tend to have slightly longer correlation lengths than ASPs. In the case of ASP-5, the 4.4 Å reflection is broader than the others, giving a correlation length of  $\sim 43$  Å. Fig. 3 shows the wide angle reflection for ASP-5 at 75°C (below the first transition temperature) and 120°C (higher than the isotropic temperature (113°C)). The wide angle reflection of ASP-5 becomes still broader at the isotropic temperature. The correlation length at 120°C is  $\sim 23$  Å, which is in the range of short-range order. Thus, ASP-5 at room temperature has somewhat more than short-range order.

Fig. 4 shows the X-ray fiber pattern of ATP-9. (The fiber patterns of the other polymers are similar.) A series of small angle reflections are located on the equator. A wide angle reflection at  $d = 4.32$  Å has increased intensity on the meridian. This is a typical fiber pattern for a  $S_B$  structure. The layer thickness, 48.0 Å, corresponds to twice the most extended side chain length (the length of  $-\text{CCH}_2\text{S}(\text{CH}_2)_6\text{SO}_2(\text{CH}_2)_9\text{H}$ :  $\sim 24$  Å). The smectic structure is a double layer formed by side chains normal to the main chain (fiber axis). The side chain conformation is probably near to all-*trans*. The smectic layer thickness increases as side chain length increases with the slope of  $\sim 2.3$  Å per methylene unit. This slope (approximately the length of two methylene units) also indicates that all the polymers studied have a double layer structure.

Table 2

Transition temperatures ( $^{\circ}\text{C}$ ) and enthalpies (J/g) (in parentheses) measured from DSC scans at a  $10^{\circ}\text{C}/\text{min}$  heating/cooling rate (Recryst: recrystallization, iso: isotropic state,  $\rho$ : packing density in the side chain)

|                                   | ASP-5                                                  | ASP-7                        | ASP-9                 | ATP-5                                                  | ATP-7                                       | ATP-9                                                  |
|-----------------------------------|--------------------------------------------------------|------------------------------|-----------------------|--------------------------------------------------------|---------------------------------------------|--------------------------------------------------------|
| Cooling                           | 58 (13)                                                | 124 (26)                     | 105 (40)<br>149 (10)  | 42 (33)                                                | 35 (9)<br>84 (32)                           | 67 (11)<br>81 (32)                                     |
| Heating                           | 80 (17)<br>113 (~5)                                    | 141 (26)                     | 112 (41)<br>153 (15)  | 60 (25)<br>63 <sub>exo</sub> (5)<br>80 (9)             | 51 (8)<br>93 (29)                           | 87 (35)<br>100 (6)                                     |
| Nature of transition <sup>a</sup> | $S_B \rightarrow S_B'$<br>$\rho \uparrow$<br>(Recryst) | $S_B \rightarrow \text{iso}$ | $S_B \rightarrow S_A$ | $S_B \rightarrow S_B'$<br>$\rho \uparrow$<br>(Recryst) | $S_B \rightarrow S_B'$<br>$\rho \downarrow$ | $S_B \rightarrow S_B'$<br>$\rho \uparrow$<br>(Recryst) |

<sup>a</sup> The transition at the first endotherm during heating.

### 3.2. Thermal properties

Several thermal transitions were observed in the ATPs and ASPs during DSC characterization. The transition temperatures and the enthalpies are summarized in Table 2. Table 2 also summarizes the structure changes that were observed. Thermal properties were strongly dependent on the side chain length and the number of sulfone groups in the side chain. It was previously reported [19] that a transition from smectic B ( $S_B$ ) to smectic B' ( $S_B'$ ) was observed at  $\sim 50^{\circ}\text{C}$  for ATP-7. At this transition, the d-spacing of the wide angle reflection increased step-wise from  $\sim 4.35$  to  $\sim 4.5$  Å without loss of long-range order in the smectic layers. This suggests that one smectic B structure changes to another slightly less dense smectic B structure at this transition. During heating, ATP-5, ATP-9 and ASP-5 have a small endothermic peak after the first melting (Fig. 5 for ATP-5). In contrast to ATP-7, these polymers densify through recrystallization. ASP-9 has two distinct transitions (at  $\sim 110^{\circ}\text{C}$  and  $\sim 150^{\circ}\text{C}$ ) during heating and cooling (Fig. 6).

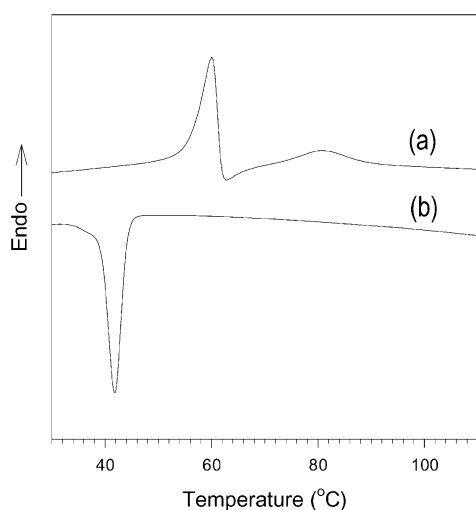


Fig. 5. DSC thermograms of ATP-5 during (a) heating and (b) cooling ( $\pm 10^{\circ}\text{C}/\text{min}$ ).

### 3.3. Recrystallization

Fig. 5 shows the DSC thermogram of ATP-5 during heating and cooling. It shows a first melting peak at  $60^{\circ}\text{C}$  ( $T_1$ ), a small exothermic peak at  $\sim 63^{\circ}\text{C}$  ( $T_{\text{ex1}}$ ) and a second melting peak at  $80^{\circ}\text{C}$  ( $T_2$ ). The exotherm indicates that recrystallization occurs after the first melting. Recrystallization phenomena in polymers having  $n$ -alkyl side chains have also been reported [3,11] from poly( $n$ -alkylethylene)s and poly( $n$ -alkylethylene oxide) [3,11]. In those studies, the crystal structure produced through recrystallization was attributed to the isotactic-rich materials, whereas the structures that melted at the first melting temperature were formed from atactic material. The smaller enthalpy at  $T_2$  (compared with that at  $T_1$ ), suggests that the extent of recrystallization is small. Fig. 7 shows the  $2\theta$  scans of X-ray powder patterns at different temperatures. The small peak at  $2\theta = 5.6^{\circ}$  (arrow in Fig. 7) comes from the Kapton film used to wrap samples during heating. The intensity of the wide angle reflection at  $d = 4.5$  Å ( $2\theta \sim 20^{\circ}$ ) decreases substantially at  $65^{\circ}\text{C}$  ( $\sim T_1$ ), but it does not disappear.

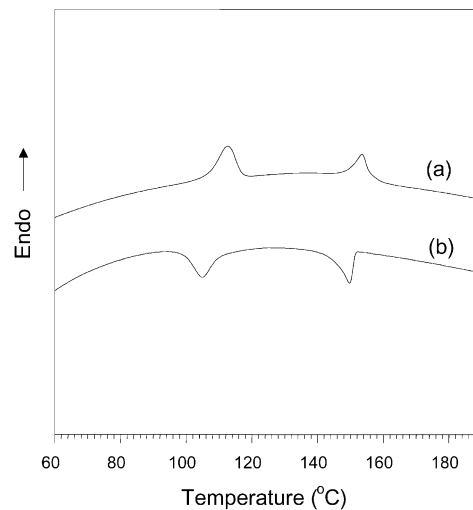


Fig. 6. DSC thermograms of ASP-9 during (a) heating and (b) cooling ( $\pm 10^{\circ}\text{C}/\text{min}$ ).

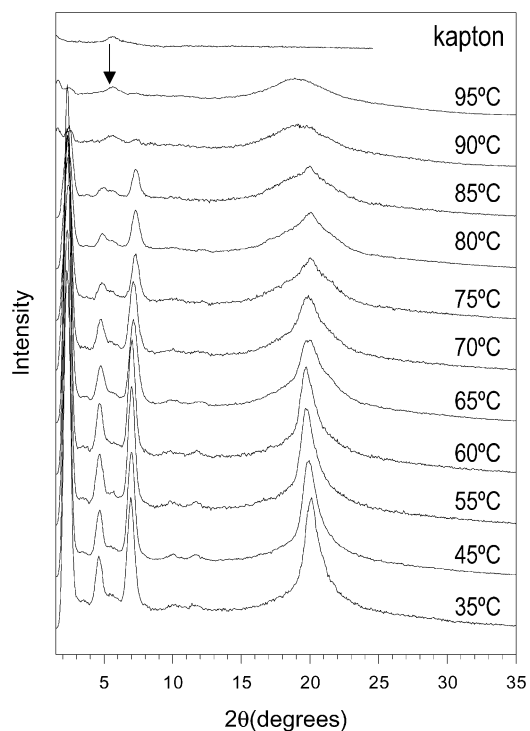


Fig. 7.  $2\theta$  scans of X-ray powder patterns of ATP-5 at different temperatures.

Fig. 8 shows d-spacings of the wide angle reflection at different temperatures.

The d-spacing for the wide angle reflection increases with temperature below  $T_1$  (thermal expansion), decreases during recrystallization, and then increases again above 75°C before disappearing at 90°C ( $\sim T_2$ ). The decrease during recrystallization indicates that crystals having more densely packed side chains were produced. In the small angle region, the d-spacing of the first Bragg peak changed only slightly above  $T_1$  ( $\sim 38$  to  $\sim 37$  Å). Thus, the structure produced through recrystallization is nearly the same as the initial structure except for the denser packing. Such

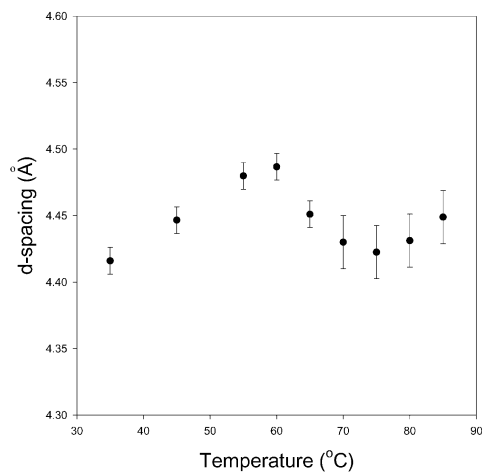


Fig. 8. d-Spacings of the wide angle reflection of ATP-5 at different temperatures.

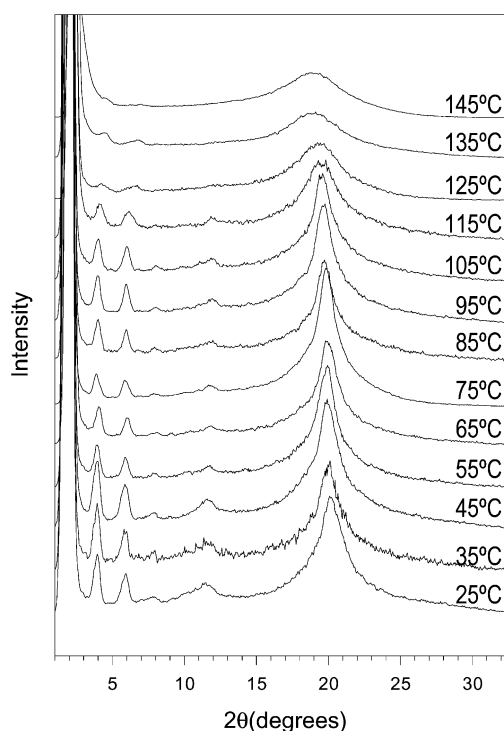


Fig. 9.  $2\theta$  scans of X-ray powder patterns of ASP-9 at different temperatures.

recrystallization behavior was also observed for ATP-9 and ASP-5, both of which have a small second melting after the first melting. Their d-spacing versus temperature plots were also similar. The enthalpy of the second melting was likewise small.

### 3.4. Smectic to smectic transition

Fig. 6 shows the DSC thermograms of ASP-9 during heating and cooling. Two transitions were observed at  $\sim 110^\circ\text{C}$  ( $T_1$ ) and  $\sim 150^\circ\text{C}$  ( $T_2$ ). The second transition temperature is quite high compared with polymers having *n*-alkyl side chains without sulfone groups. This transition is not simple melting of the *n*-alkyl side chains and is probably related to strong interactions between sulfone groups. Recently, (*n*-hexadecylthio)methyl-substituted poly(oxyethylene) was synthesized. This polymer has a flexible thioether ( $-\text{S}-$ ) linkage in the side chain but no sulfone group. Although, the side chain length in this polymer (18 atoms) is very close to that of ASP-9 (also 18 atoms), the isotropic temperature was only  $\sim 50^\circ\text{C}$ , much lower than that of ASP-9. This is close to the melting temperatures of polymers with long alkyl tails such as poly(*n*-alkylethylene) or poly(*n*-alkylethylene oxide) [3,11]. [The isotropic temperatures of poly(octadecylethylene) and poly(octadecylethylene oxide) are  $\sim 80^\circ\text{C}$  and  $\sim 65^\circ\text{C}$ , respectively.]

Fig. 9 shows the X-ray powder patterns from ASP-9 during heating and Fig. 10 shows the observed d-spacing and correlation length of the wide angle reflection at different temperatures. Below  $105^\circ\text{C}$  ( $\sim T_1$ ), a series of sharp

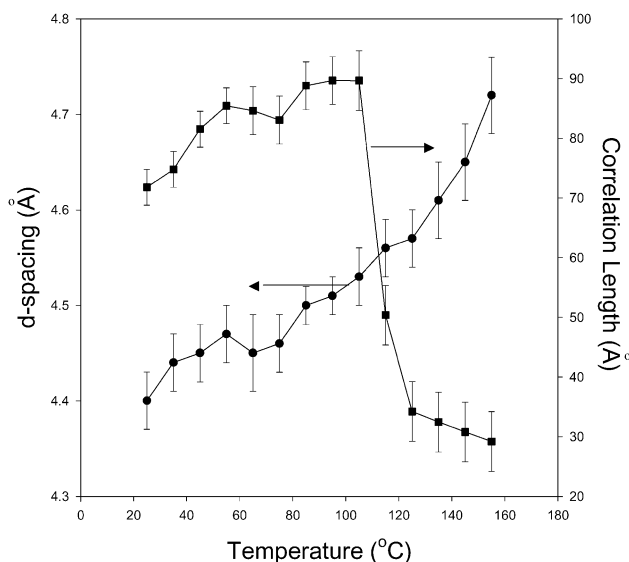


Fig. 10. The observed d-spacings (●) and the correlation lengths (■) determined from the wide angle reflection of ASP-9.

small angle reflections and a wide angle reflection at  $d = 4.4 \text{ \AA}$  were observed (as mentioned before) from the  $S_B$  structure. The d-spacing of the wide angle reflection increased monotonically with temperature. The correlation length also increased somewhat during heating below  $T_1$ . At  $115^\circ\text{C}$  ( $\sim T_1$ ), the wide angle reflection became broad and the correlation length decreased from  $\sim 80$  to  $\sim 30 \text{ \AA}$ . In the small angle region, a series of reflections was still observed (Fig. 9) although their intensity decreased substantially. Apparently, some smectic organization remains above this transition but the layer thickness decreases from  $\sim 46$  to  $\sim 40 \text{ \AA}$  at  $T_1$ . This decrease of layer thickness could be attributed to the partial collapse of the extended conformation of side chains or to tilting within the layers. Whatever the cause, the order in the smectic layers diminishes and the  $S_B$  structure converts to a less ordered smectic structure (probably smectic A) at  $T_1$ . This type of transition is not observed in polymers with  $n$ -alkyl side chains and therefore it appears to be an effect of having the strong dipoles in the side chain.

No birefringence was detected in ASP-9 above  $T_2$  ( $150^\circ\text{C}$ ), indicating that this transition is to an isotropic phase. ATP-9, which has a similar chain length but only a single sulfone group in the middle of the side chain, has an isotropic temperature at  $87^\circ\text{C}$ , much less than that of ASP-9 (two sulfone groups) and ASE-16 (isotropic temperature,  $154^\circ\text{C}$ , one sulfone group near the backbone). No smectic B to smectic A transition was seen for ATP-9. Both the number and placement of strong dipoles have an effect on the thermal stability of the mesophase in these materials.

#### 4. Conclusions

The structures of  $(-\text{OCH}_2\text{CHR}-)$  with  $\text{R} =$

$\text{CH}_2\text{S}(\text{CH}_2)_6\text{SO}_2(\text{CH}_2)_M\text{H}$  (ATP-M;  $M = 5, 7, 9$ ) and  $\text{R} = \text{CH}_2\text{SO}_2(\text{CH}_2)_6\text{SO}_2(\text{CH}_2)_M\text{H}$  (ASP-M;  $M = 5, 7, 9$ ) were studied using X-ray diffraction and differential scanning calorimetry. The X-ray patterns of all ATPs and ASPs studied show a series of ordered reflections in the small angle region and a sharp reflection at  $d = \sim 4.4 \text{ \AA}$ . The small angle reflections were located on the equator. The wide angle reflection had increased intensity on the meridian in the X-ray fiber patterns, characteristic of a smectic layer structure. The observed smectic layer thickness corresponds to twice the extended side chain length and increases linearly with side chain length with slope of  $\sim 2.3 \text{ \AA}$  per a methylene spacer. This indicates that all ASPs and ATPs studied have a double layer structure comprised of side chains normal to the main chain. The correlation lengths measured from the wide angle reflection are in the range of  $80 \pm 10 \text{ \AA}$  except for ATP-5 ( $\sim 40 \text{ \AA}$ ). These values indicate that quasi-long-range order exists in the smectic layers and their structures can be defined as smectic B ( $S_B$ ). The d-spacing of the wide angle reflection,  $4.4 \text{ \AA}$ , indicates that paraffinic side chain crystallization of  $n$ -alkyl groups does not occur. Instead, the smectic mesophases develop through dipole–dipole interactions of sulfone groups in the side chains. Recrystallization was observed in the case of ATP-5, ASP-5 and ATP-9. The structures produced during recrystallization have more densely packed side chains in the smectic layers than before the first melting. ASP-9 showed a transition at  $\sim 110^\circ\text{C}$  before the isotropic temperature at  $\sim 150^\circ\text{C}$ . The correlation length of the wide angle reflection decreased from  $\sim 80$  to  $\sim 30 \text{ \AA}$  at this transition and the layer thickness decreased from  $46$  to  $40 \text{ \AA}$ . The order in the smectic layers was lost and the  $S_B$  structure became less ordered (probably converting to  $S_A$ ) at this transition. This transition was not observed for ATP-9, suggesting that the  $S_A$  structure for ASP-9 (above  $T_1$ ) may be due to the dipole–dipole interactions of sulfone groups closer to the main chain.

#### Acknowledgements

S.-Y. Park acknowledges support from the Air Force Office of Scientific Research for an NRC Postdoctoral Research Associateship. Financial support of this work by the Korea Science and Engineering Foundation through the Hyperstructured Organic Materials Research Center is gratefully acknowledged by J.C. Lee.

#### References

- [1] Yokota K, Hirabayashi T. *Polymer J* 1986;18:177.
- [2] Andruzzi F, Hvisted S, Paci M. *Polymer* 1994;35:4449.
- [3] Magagnini PL, Andruzzi F, Benetti GF. *Macromolecules* 1980;13:12.
- [4] Yokota K, Kougo T, Hirabayashi T. *Polymer J* 1983;15:891.
- [5] Tsiourvas D, Paleos CM, Skoulios A. *Macromolecules* 1997;30:7191.
- [6] Jordan Jr EF, Feldeisen DW, Wrigley AN. *J Polym Sci Part A-1* 1971;9:1835.

- [7] Jordan Jr EF, Artymyshyn B, Specca A, Wrigley AN. *J Polym Sci Part A-1* 1971;9:3349.
- [8] Hsieh HWS, Post B, Morawetz H. *J Polym Sci Polym Phys Ed* 1976;14:1241.
- [9] Watanabe J, Ono H, Uematsu I, Abe A. *Macromolecules* 1985;18:2141.
- [10] Ganalezdela-Campa JI, Barrales-Rienda JM. *J Polym Sci Polym Phys Ed* 1980;18:1919.
- [11] Andruzzi F, Lupinacci D, Magagnini PL. *Macromolecules* 1980;13:15.
- [12] Rehberg CE, Fischer CH. *J Am Chem Soc* 1944;66:1203.
- [13] Kaufman HS, Sacher A, Alfrey Jr T, Fankuchen I. *J Am Chem Soc* 1948;76:6280.
- [14] Plate NA, Shibaev P, Petrukhin BS, Zubov YA, Kargin VA. *J Polym Sci Part A-1* 1971;9:2291.
- [15] Plate NA, Shibaev VP. *J Polym Sci Macromol Rev* 1974;8:117.
- [16] O'Donnell JH. PhD Thesis, Leeds University, 1963.
- [17] Lee JC, Litt MH, Rogers CE. *Macromolecules* 1998;31:2440.
- [18] Lee JC, Kim YG, Lee HB, Oh K, Park SY, Farmer BL. *ACS Polymer Preprints* 2000;41(2):1603.
- [19] Lee JC, Oh K, Lee HB, Kim YG, Jho JY, Kwak SY, Park SY, Farmer BL. *Macromol Rapid Commun* 2001;22:815.
- [20] Yoon Y, Zhang A, Ho RM, Chengs ZD, Percec V, Chu P. *Macromolecules* 1996;29:294.
- [21] Zheng RQ, Chen EQ, Chengs ZD, Xie F, Yan D, He T, Percec V, Chu P, Ungar G. *Macromolecules* 1999;32:3574.